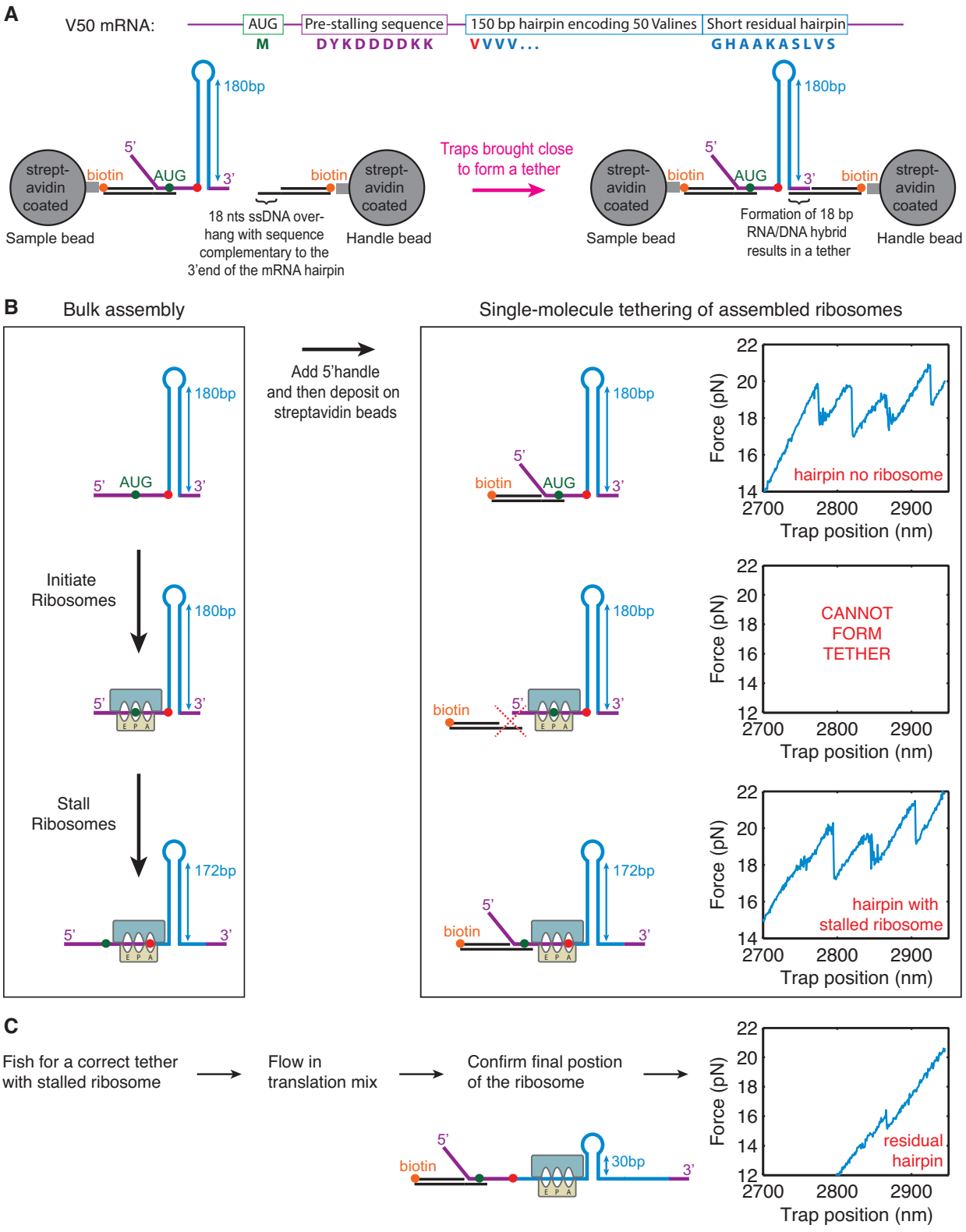

Figure S1. Assembly and tethering of ribosome stalled complexes, Related to Figure 1

Figure S1. Assembly and tethering of ribosome stalled complexes, Related to Figure 1 (contd.)

(A) Tethering geometry: a 2.5 kb double-stranded DNA handle with biotin on one end and 20 nts of single-stranded DNA on the other end is annealed to complementary 20 nts at the 5' side of an mRNA hairpin and is deposited on streptavidin coated beads – this assembly is called the sample bead. A different 2.5 kb double-stranded DNA handle with biotin on one end and 18 nts of single-stranded DNA overhang that is complementary to the 3' side of the mRNA on the other end is deposited on streptavidin coated beads – this assembly is called the handle bead. A sample and a handle bead are caught in two optical traps respectively and as they are brought together, the formation of an RNA/DNA hybrid between the 18 nts of ssDNA on the handle bead and the 3' end of the mRNA hairpin results in a 'tether' in our optical tweezers setup.

(B) Sample preparation overview: *Left,* bulk assembly of ribosome-stalled complexes: First, ribosomes are initiated on the mRNA upstream from the hairpin. Then, by supplying amino acids D, Y and K, the ribosomes are stalled when the first valine codon reaches the P-site of the ribosome. At this point, the foot-print of the ribosome results in the opening of 8 base-pairs of the hairpin. This bulk stalling strategy results in three types of complexes: 1) mRNA only – mRNA that harbors no ribosome, 2) initiation complexes – mRNA where the ribosome initiated successfully but did not move past the start codon to stall at the valine codon, and 3) stalled complexes – mRNA with ribosome correctly stalled with the valine codon in the P-site. Then, 5' handle with 20 nts of single-stranded DNA that is complementary to 20 nts of the 5' side of an mRNA hairpin is added. *Right,* Tethering of the three complexes formed in bulk and their unfolding signatures: the 5' handle can bind only to the mRNA only and stalled complexes. In the case of mRNA only, there is no ribosome and hence the hairpin is fully closed and results in four rips in the force-extension curves. As opposed to that, in the stalled complexes, the foot-print of the ribosome has partially opened the hairpin (by 8 bps) and results in three rips with the first rip displaying a characteristic shoulder. These unfolding signatures allow us to correctly identify a ribosome-stalled complex on the tweezers.

(C) The unfolding signature of the short residual hairpin remaining at the end of translation is shown. If the ribosome stalled before the residual hairpin, the unfolding signature can be used to accurately determine the exact stopping position of the ribosome.

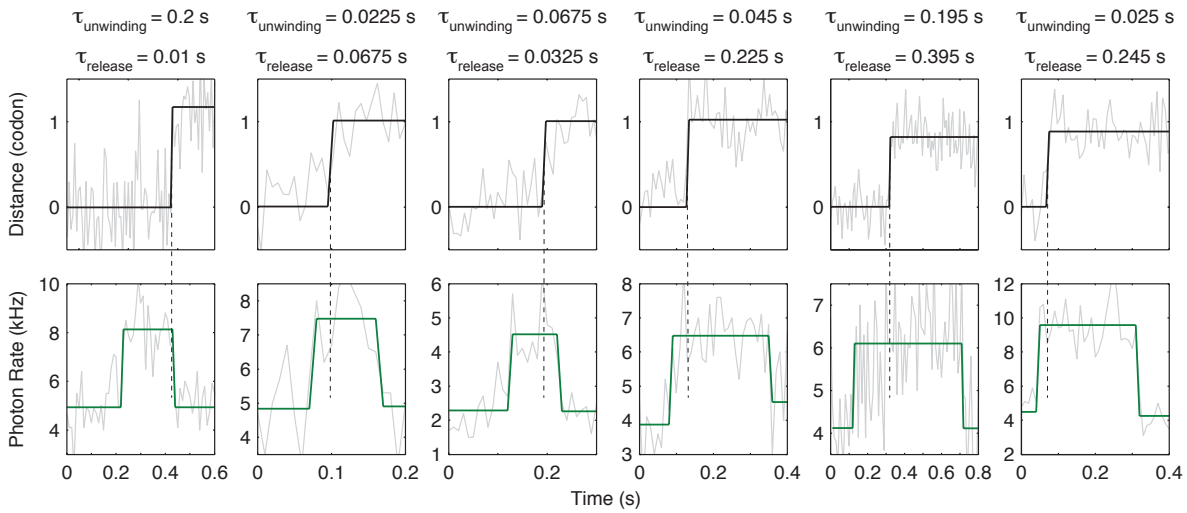

Figure S2. Zoomed-in translocation events when hairpin is held under high force, Related to Figure 1

Top panel: optical tweezers channel – 133 Hz data (shown in grey) is fit as described in Methods, fit results are shown as solid black lines; Bottom panel: fluorescence channel – 100 Hz data (shown in grey) is fit as described in Methods, fit results are shown as solid green lines. Concentration of Cy3-labeled-EF-G is 10 nM.

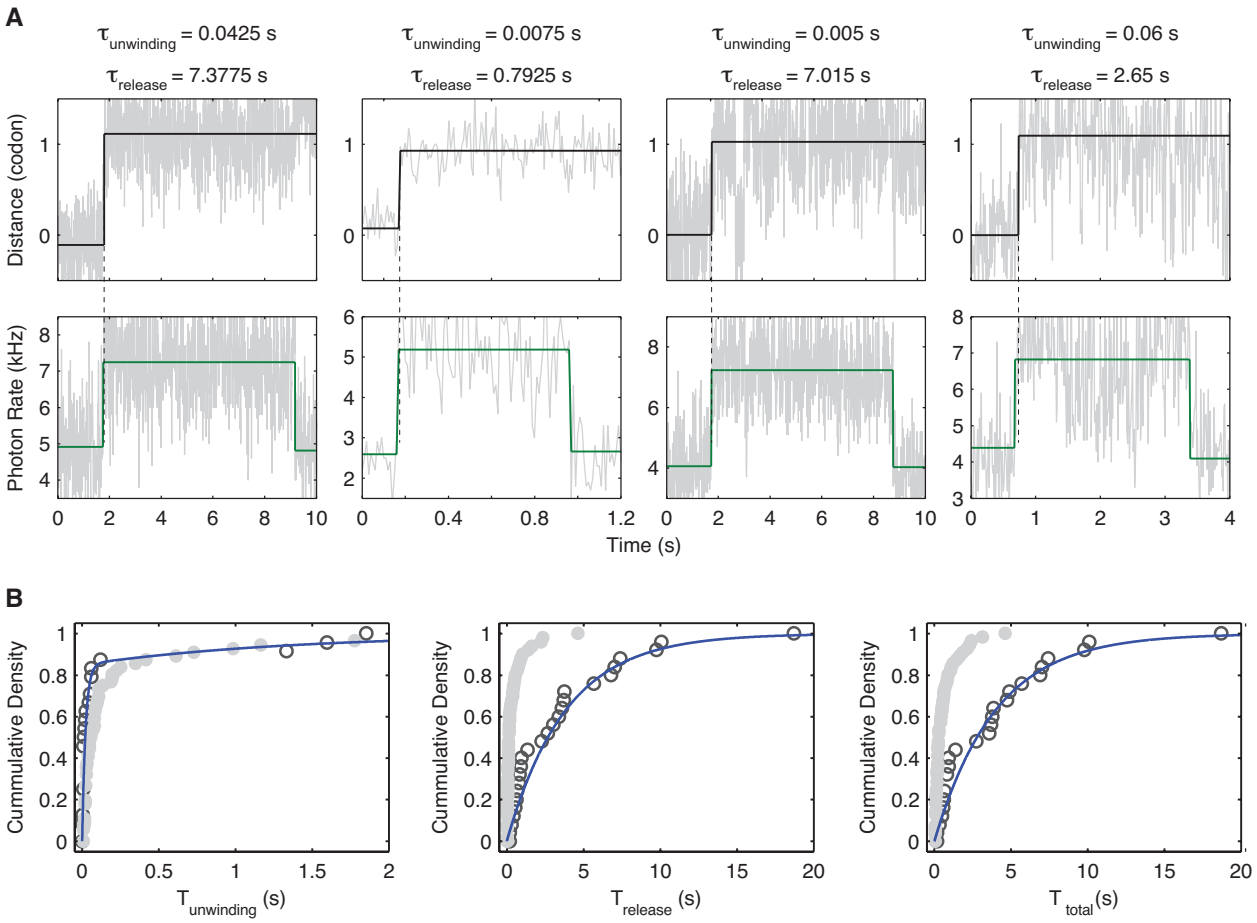

Figure S3. Hairpin opening and EF-G binding and release measurements in the presence of antibiotic fusidic acid, Related to Figure 2

(A) Hairpin held at high force (> 13pN, weak hairpin) in the presence of 200 μM fusidic acid and 10 nM Cy3-labeled-EF-G. Top panel: optical tweezers channel – 133 Hz data (shown in grey) is fit as described in Methods, fit results are shown as solid black lines; bottom panel: fluorescence channel – 100 Hz data (shown in grey) is fit as described in Methods, fit results are shown as solid green lines.

(B) Cumulative density distributions of time between EF-G binding and unwinding ($\tau_{\text{unwinding}}$), time between unwinding and EF-G release (τ_{release}) and the total time EF-G is bound to the ribosome ($\tau_{\text{total}} = \tau_{\text{unwinding}} + \tau_{\text{release}}$). Black open circles represent data collected with 200 μM fusidic acid (n = 25 events, 13 molecules) and grey filled circle represent data without fusidic acid (n = 55 events, 9 molecules). Blue lines are fits to the cumulative distribution summarized in Table S1.

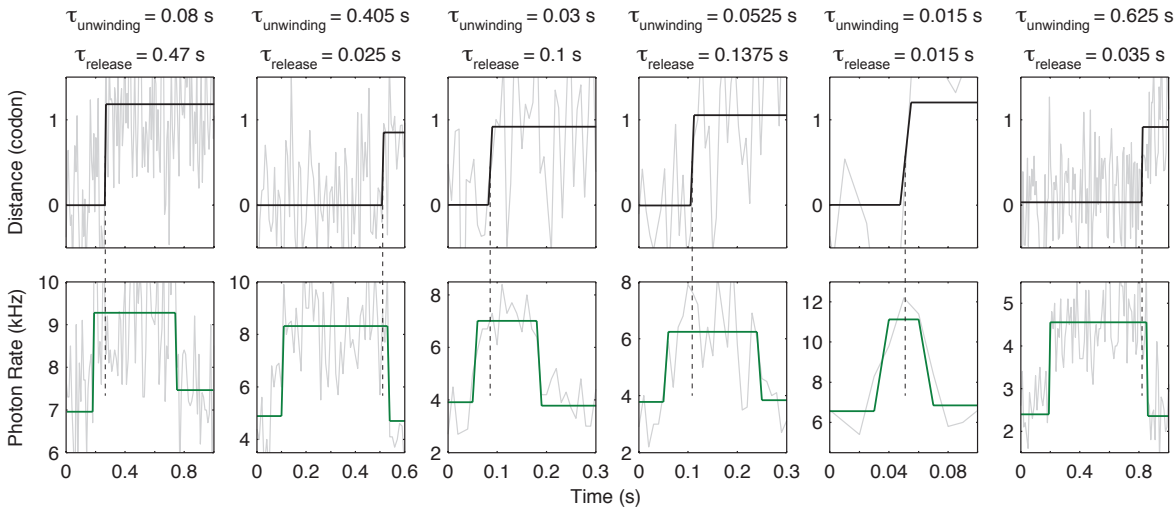

Figure S4. Zoomed-in translocation events when hairpin is held under low force, Related to Figure 3

Top panel: optical tweezers channel – 133 Hz data (shown in grey) is fit as described in Methods, fit results are shown as solid black lines; Bottom panel: fluorescence channel – 100 Hz data (shown in grey) is fit as described in Methods, fit results are shown as solid green lines. Concentration of Cy3-labeled-EF-G is 10 nM.

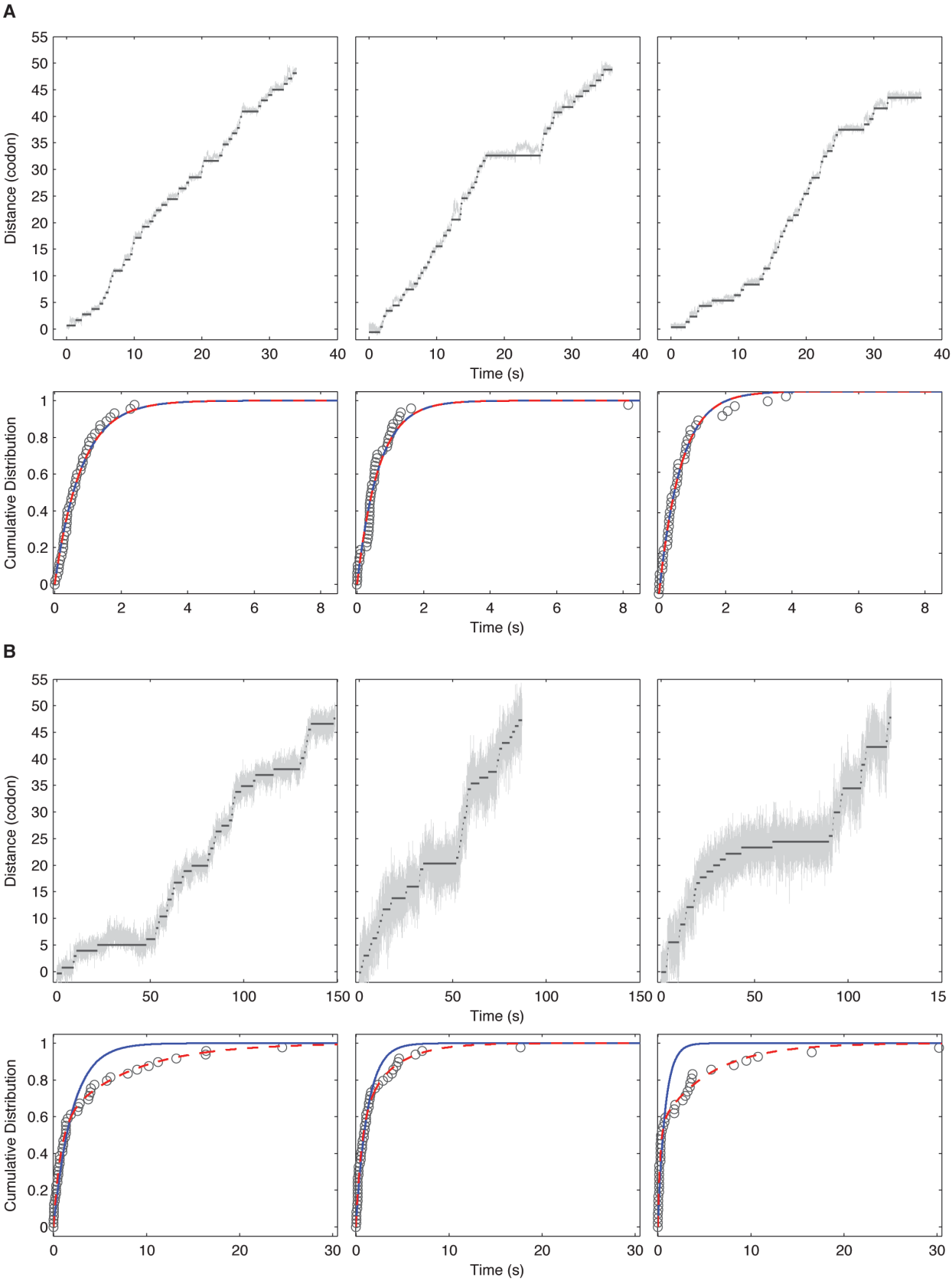

Figure S5. Bi-exponential distribution is shown in individual traces, Related to Figure 4

Figure S5. Bi-exponential distribution is shown in individual traces, Related to Figure 4 (contd.)

(A) Top panel: examples of single-ribosome optical tweezers trajectories of hairpin opening at 10 μM EF-G (high force > 13 pN, weak hairpin). Black lines represent HMM fit for each step. Note that the HMM fit is capable of ignoring reversible fluctuations at the hairpin base (middle trace, long dwell around t = 20 s). Bottom panel: cumulative density distribution of the respective traces. Single exponential (blue line) and bi-exponential (red line) fits are shown.

(B) Same as (A) but at low force < 7 pN, strong hairpin. Notice the difference in fit quality between single and bi-exponential fit (blue and red lines respectively) in the cumulative density distributions.

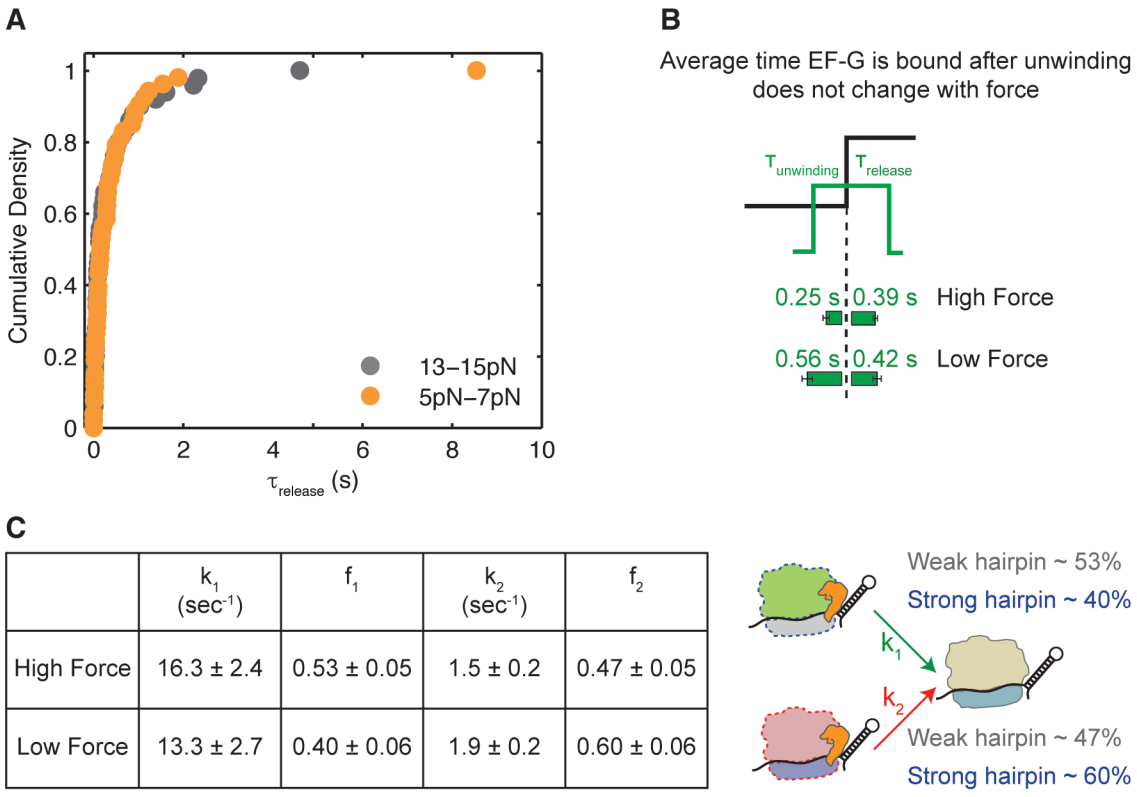

	k_1 (sec^{-1})	f_1	k_2 (sec^{-1})	f_2
High Force	16.3 ± 2.4	0.53 ± 0.05	1.5 ± 0.2	0.47 ± 0.05
Low Force	13.3 ± 2.7	0.40 ± 0.06	1.9 ± 0.2	0.60 ± 0.06

Figure S6. $\tau_{release}$ follows a biphasic distribution that is insensitive to force, Related to Figure 4

(A) Cumulative density distribution of $\tau_{release}$ at high force (> 13pN, weak hairpin, n = 55 events from 9 molecules) and low force (< 7 pN, strong hairpin, n = 62 events, 14 molecules) in presence of 10 nM Cy3-labeled-EF-G.

(B) Average residence times of EF-G before and after hairpin opening. Errors represent SEM.

(C) Results of fits to $\tau_{release}$ at high force (> 13pN, weak hairpin) and low force (< 7 pN, strong hairpin). Errors represent 95% confidence intervals.

Table S1. Summary of bi-exponential fits at various forces and EF-G concentrations, Related to Figures 1-4

k_{dwell}

Force (pN)	[EF-G]	k_1(s^{-1})	f_1(%)	k_2(s^{-1})	f_2(%)
15	10 μM	1.1 ± 0.03	91 ± 2	0.02 ± 0.06	9 ± 2
15	1 μM	1.19 ± 0.03	84 ± 2	0.23 ± 0.03	16 ± 2
15	100 nM	0.66 ± 0.03	96 ± 1	0.04 ± 0.02	4 ± 1
15	30 nM	0.53 ± 0.01	100	x	x
10	10 μM	0.75 ± 0.01	97 ± 1	0.05 ± 0.04	3 ± 1
5	10 μM	0.71 ± 0.03	69 ± 2	0.19 ± 0.01	31 ± 2
5	1 μM	0.61 ± 0.03	56 ± 4	0.17 ± 0.01	44 ± 4
5	100 nM	0.41 ± 0.01	76 ± 2	0.08 ± 0.01	24 ± 2
5	30 nM	0.37 ± 0.13	29 ± 29	0.18 ± 0.03	71 ± 29
3	10 μM	1.1 ± 0.04	51 ± 1	0.16 ± 0.01	49 ± 1

$k_{\text{unwinding}}$ ([EF-G] = 10 nM)

Force (pN)	Antibiotic	k_1(s^{-1})	f_1(%)	k_2(s^{-1})	f_2(%)
14 – 17	x	21.13 ± 4.80	92 ± 12	1.00 ± 3.82	8 ± 12
12 – 14	x	27.53 ± 4.70	76 ± 8	1.89 ± 1.34	24 ± 8
7 – 9	x	35.48 ± 10.38	61 ± 12	3.17 ± 1.57	39 ± 12
5 – 8	x	12.7 ± 1.45	62 ± 4	0.89 ± 0.17	38 ± 4
13 – 15	Fusidic acid	25.4 ± 15.4	96 ± 29	0.23 ± 0.03	4 ± 29

Data S1. Alternate kinetic schemes, Related to Figure 4

The time the ribosome spends at a particular codon before moving to the next codon is defined as τ_{dwell}

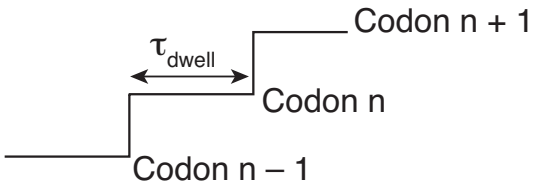

The simplest model to describe the movement of ribosome from codon n to codon $n+1$ can be described as:

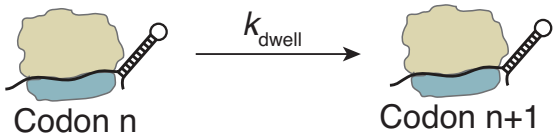

In this case, the movement of ribosome at each codon is given by a single rate limiting event k_{dwell}. The probability distribution of observing a dwell of time t would be given by:

$$P(t) = k_{\text{dwell}} \cdot e^{-k_{\text{dwell}} \cdot t}$$

The cumulative probability of the above distribution is given by:

$$F(t) = 1 - e^{-k_{\text{dwell}} \cdot t}$$

While this distribution fits ~90% of the data at high force, it does not fit data at low force (Figure 4A).

The data instead fits very well to a mixture of two exponential distribution given by:

$$P(t) = f_1 \cdot k_1 \cdot e^{-k_1 \cdot t} + f_2 \cdot k_2 \cdot e^{-k_2 \cdot t}$$

where k_1 and k_2 are the rates of the two exponential distributions, f_1 and f_2 are the relative populations of the two exponential distributions, and $f_1 + f_2 = 1$

The cumulative probability of the above distribution is given by:

$$F(t) = 1 - f_1 \cdot e^{-k_1 \cdot t} - f_2 \cdot e^{-k_2 \cdot t}$$

The dwell time distribution fits a mixture of exponentials (bi-exponential) at both high and low forces. The result of the fit gives k_1, k_2 and f_2 (Figures 4B and 4C). We have $f_1 = 1 - f_2$.

For a bi-exponential distribution, a simple scheme where the ribosome goes into an off-pathway *inactive* state in presence of a barrier could be proposed:

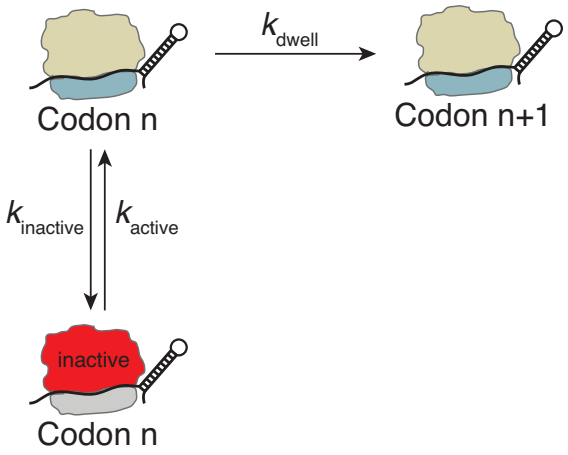

In order to solve this scheme exactly, let A be the probability of being in the active state at codon n and I the probability of being in the inactive state.

The following system of equation holds:

$$\frac{dA}{dt} = -(k_{\text{dwell}} + k_{\text{inactive}})A + k_{\text{active}}I \qquad (1)$$

$$\frac{dI}{dt} = -k_{\text{active}}I + k_{\text{inactive}}A \qquad (2)$$

Then Equation (1) can be rearranged as:

$$I = \frac{1}{k_{\text{active}}}\frac{dA}{dt} + \frac{(k_{\text{dwell}} + k_{\text{inactive}})}{k_{\text{active}}}A$$

and then be plugged into Equation (2) to yield:

$$\frac{d^2A}{dt^2} + (k_{\text{dwell}} + k_{\text{inactive}} + k_{\text{active}})\frac{dA}{dt} + k_{\text{dwell}}k_{\text{active}}A = 0$$

This is a second order differential equation and the eigenvalues are:

$$\lambda_{+/-} = \frac{-(k_{\text{dwell}} + k_{\text{inactive}} + k_{\text{active}}) \pm \sqrt{(k_{\text{dwell}} + k_{\text{inactive}} + k_{\text{active}})^2 - 4k_{\text{dwell}}k_{\text{active}}}}{2}$$

and A and I are linear combinations of $\exp(\lambda_+ t)$ and $\exp(\lambda_- t)$.

At $t = 0$, $I = 0$; thus

$$I(t) = C(\exp(\lambda_+ t) - \exp(\lambda_- t))$$

and then, from Eq (2), we have,

$$A(t) = \frac{1}{k_{\text{inactive}}}\frac{dI}{dt} + \frac{k_{\text{active}}}{k_{\text{inactive}}} I = C\left(\frac{\lambda_+ + k_{\text{active}}}{k_{\text{inactive}}}\exp(\lambda_+ t) - \frac{\lambda_- + k_{\text{active}}}{k_{\text{inactive}}}\exp(\lambda_- t)\right)$$

The probability of being either in the active or the inactive state at codon n, which is also the distribution for the dwell time at codon n, is thus

$$A(t) + I(t) = C\left(\frac{\lambda_+ + k_{\text{active}} + k_{\text{inactive}}}{k_{\text{inactive}}}\exp(\lambda_+ t) - \frac{\lambda_- + k_{\text{active}} + k_{\text{inactive}}}{k_{\text{inactive}}}\exp(\lambda_- t)\right)$$

i.e., it is biexponentially distributed. Importantly, in this model, the ratio between the populations of the two exponentials, $-(\lambda_+ + k_{\text{active}} + k_{\text{inactive}})/(\lambda_- + k_{\text{active}} + k_{\text{inactive}})$, is not independent of the ratio between the rates of the two exponentials, λ_+/λ_-: it is generally not possible to change the ratio between the exponentials' populations without changing the observed exponential rates. This is not consistent with our measurements, which show that a change in force causes a change in the population ratio without modifying the rates.

Therefore, we need a scheme where the pathway populations are determined independently of and prior to the rate-limiting event in the two pathways:

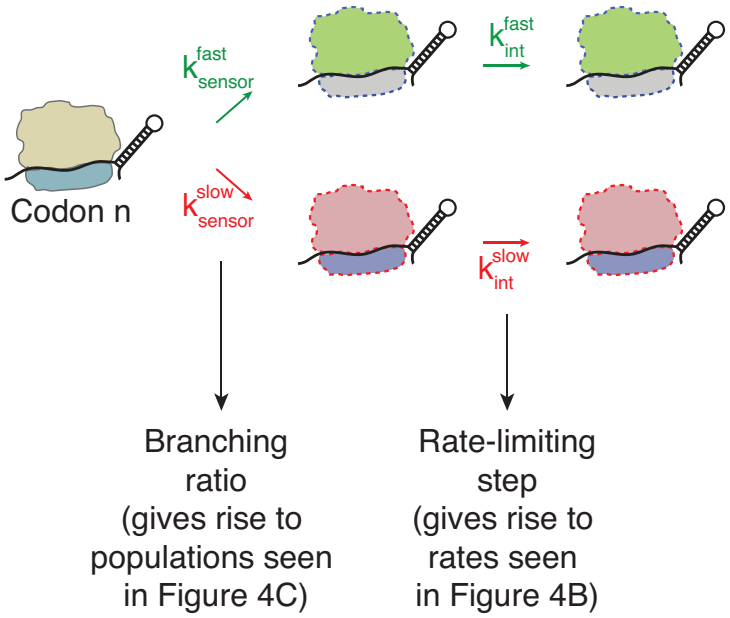

Now, this bifurcation could occur a) prior to EF-G binding or after EF-G release from previous cycle, b) prior to EF-G binding through unwinding, or c) after unwinding through EF-G release:

a) Pathway bifurcation and resetting occurs before EF-G binding or after EF-G release from previous cycle

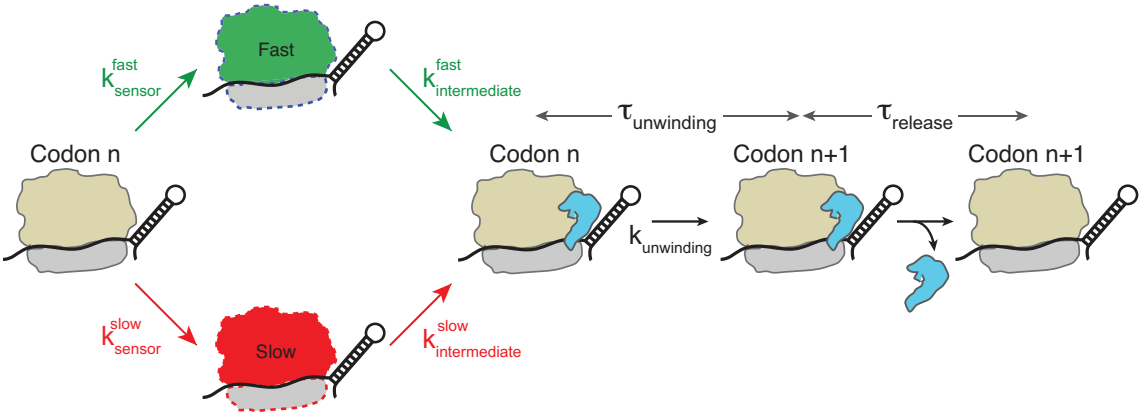

b) Pathway bifurcation occurs before EF-G binding and resets upon hairpin opening

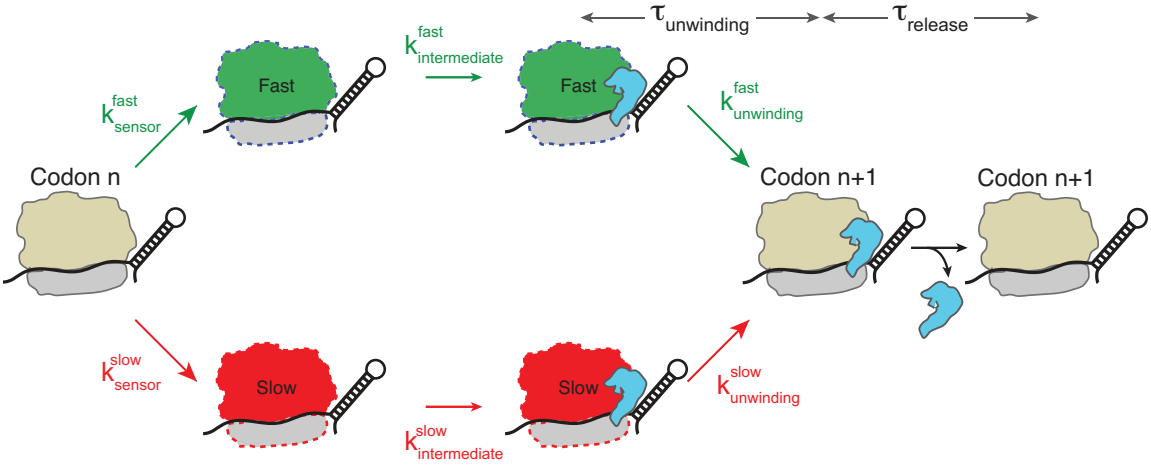

c) Pathway bifurcation and resetting occurs after hairpin opening

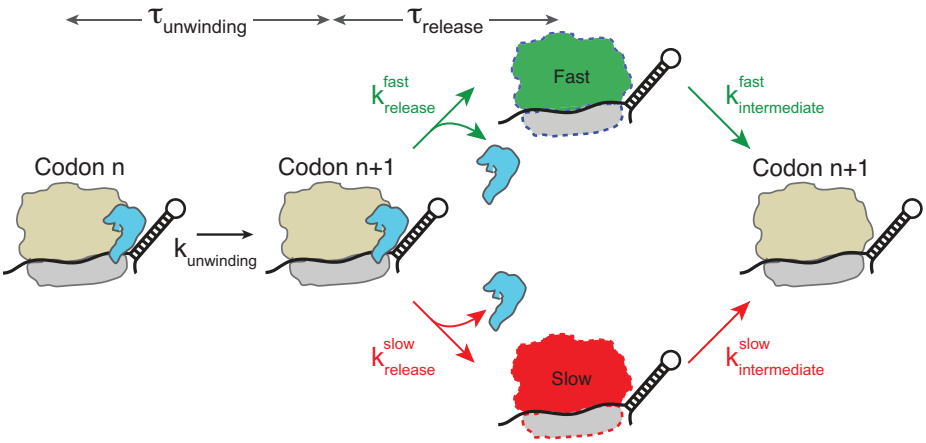

One possible way to distinguish these schemes is by looking at the distribution of $\tau_{\mathrm{unwinding}}$, time from EF-G binding to unwinding (Figure 4D). In a), neither $\tau_{\mathrm{unwinding}}$ or τ_{release} would have a bi-exponential distribution where the populations of the two distributions are force-sensitive. In b), $\tau_{\mathrm{unwinding}}$ would be described by a bi-exponential where the populations are sensitive to force in a manner similar to that observed for τ_{dwell}. In c), τ_{release} would be described by a bi-exponential where the populations are sensitive to force in a manner similar to that observed for τ_{dwell}. In our experiments, we observe that the distribution $\tau_{\mathrm{unwinding}}$ is also best described by a mixture of two exponentials where the rates are force-insensitive (Figure 4E) but the pathway populations are force-dependent (Figure 4F). Moreover, τ_{release}, time from unwinding to EF-G release (Figure S6) is insensitive to force and therefore we propose that the bifurcated pathway has reset prior to release and therefore favor model b).